Vol. 46, No. 2 (2024) 217-235, DOI: 10.24874/ti.1532.08.23.10

Tribology in Industry

www.tribology.rs

RESEARCH

# Tribological Behaviour of Short Carbon Fiber Reinforced Polyethersulfone Composites with PTW Filler

B. Harshavardhan[a], R. Ravishankar[b], Arun C. Dixit U.[c], D. Anandraj[a]

[a]*Department of Mechanical Engineering, The National Institute of Engineering, Mysuru, Karnataka-570 008, India,*
[b]*Department of Mechanical Engineering, Sri Jayachamarajendra College of Engineering, Mysuru-570 006, India,*
[c]*Department of Mechanical Engineering, Vidyavardhaka College of Engineering, Mysuru, Karnataka -570 002, India.*

Keywords:

*Polyethersulfone*
*Short carbon fibers*
*Potassium titanate whisker*
*Central composite design*
*Pin-on-disc*
*Specific wear rate*
*Coefficient of friction*

* Corresponding author:

*B. Harshavardhan*
*E-mail: harshavardhanb@nie.ac.in*

*Received: 14 August 2023*
*Revised: 27 September 2023*
*Accepted: 24 October 2023*

A B S T R A C T

*In various applications like bearings, gear pairs, and brake pads, understanding how polymer composites interact with harder counterparts during sliding motions is crucial. A challenge arises from the heat generated during sliding friction, which has the potential to raise the contact temperature. This temperature increase, if it exceeds the material's glass transition temperature, can compromise the thermal stability of the composites, leading to rapid material wear. In the present investigation, dry sliding wear test was performed on 25 wt. % of short carbon fiber (SCF) reinforced polyethersulfone (PES) composites filled with 2.5 and 5.0 wt. % of potassium titanate whisker (PTW) using pin-on-disc tribometer. Wear test was planned and executed according to the experiment design formulations obtained by central composite design method. Contact temperature at the interface between composite pin and steel disc was monitored with an infrared thermal camera. Wear resistance was found to increase with the addition of fibers and fillers. PTW filled composites exhibited minimum wear with maximum coefficient of friction. Morphology studies were carried out on worn surfaces of the composites using scanning electron microscope to identify and describe the mechanism of wear involved. This investigation sheds light on the intricate behavior of polymer composites during sliding interactions.*



## 1. INTRODUCTION

Fiber reinforced polymer composites are preferred for tribological applications due to their high strength, low coefficient of friction, self lubrication and low wear rate [1]. Polyethersulfone is one of the best engineering thermoplastic materials suitable for applications such as bearings, bearing bushes, gears etc. due to its high glass transition temperature (220 °C) and melting temperature (330 °C) [2]. Synthetic fibers such as glass fibers, carbon fibers, aramide fibers, basalt fibers etc. have been extensively used to improve the mechanical strength of the

engineering thermoplastic polymers such as polyamide (PA), polysulfone (PS), polybutylenetherapthalate (PBT), polyethersulfone (PES), polyphenoylsulfide (PPS), polyetheretherketone (PEEK) [3]. Many researchers investigated and proved that surface modification of fibers improved the mechanical performance of polymer composites. Mechanical properties of the PES/SCF composites were improved by coating the SCFs with phenol-formaldehyde (PF) resin. Enhancement in interface adhesion between PES and SCF was noticed in the scanning electron microscope images [4]. Graphene oxide (GO) was used as the coating agent on SCFs and optimum mechanical performance was observed at 0.5 wt. % of GO due to the enhancement in interfacial adhesion [5]. Tensile strength of ABS/PMMA composites increased slightly with 5 wt. % of PTW and thermal stability was enhanced [6]. Few studies were focused on the effect of fiber reinforcements on tribological behaviour of polyethersulfone composites. Effect of different volume fraction of short glass fibers (SGF) and short carbon fibers (SCF) separately reinforced into PES on tribological properties were studied [7]. Wear resistance of SGF and SCF reinforced PES composites greatly improved. Maximum reduction in wear rate of PES composite was observed due to the addition of SCF than the SGF. Also, maximum drop in coefficient of friction was observed in the case of addition of SCF. SGF/PES was found to be superior when cost is the primary consideration, otherwise SCF/PES found more effective.

Role of solid lubricants such as molybdenum disulfide ($MoS_2$), polytetrafluroethylene (PTFE), ultra high molecular weight polyethylene (UHMWPE), potassium titanate whisker (PTW) is crucial role in enhancing the wear resistance of the polymer composites. PES with 18 wt. % of short glass fibers reinforcement were filled with 2 wt. % of $MoS_2$ and PTFE fillers separately and enhancement in the adhesive wear performance of composites by an order of two was observed [8]. PA6/$TiO_2$ composite was filled with three solid lubricants namely PTFE, $MoS_2$, and UHMWPE in various proportions and wear studies were performed on those hybrid composites. Wear studies revealed that tribological performance of composite filled with $MoS_2$ and UHMWPE was better than other filler combinations [9].

Potassium titanate whisker was employed as a prospective inorganic filler with the aim of enhancing the wear resistance of thermoplastics. Glass fibers and PTW were filled separately in the proportions 1, 3 and 5 wt. % in PTFE/PEEK composites and observed that coefficient of friction of the PTW series was slightly lower than that of the GF series at the same additive ratio, while the wear rate was the opposite, indicating that the wear resistance of GF was better than PTW [10]. PTW enhanced the mechanical strength as well as wear resistance of epoxy composites [11–14]. Tribological and mechanical performance of PTFE/PEEK composites filled with un-modified and modified PTW with n-octadecyltrichlorosilane were comparatively studied and reported that modified PTW showed higher wear resistance than the unfilled ones [15].

Taguchi experimental design has been widely used to perform various kinds of tribological tests on metal, polymer and ceramic matrix composites [16-17]. Response surface method is also a powerful statistical and mathematical tool to predict the effect of wear test parameters on the specific wear rate [18-19].

In the current research work, in order to understand the effect of PTW on the tribological properties of PES/SCF composites, test samples were prepared by filling 2.5 wt.% and 5 wt.% of PTW into PES/SCF composites and dry sliding wear test was conducted on the samples for various loads and velocities as per central composite experimental design methodology. It was aimed to monitor contact temperature in addition to friction and wear during the tribo-test.

## 2. MATERIALS AND METHODS

### 2.1 Materials

In this section, the various components of the composite materials are delineated. The matrix material selected is Polyethersulfone (PES), an engineering thermoplastic known for its amorphous nature and high-performance attributes. To reinforce the composite, short carbon fibers (SCF) were incorporated, possessing a moderate tensile modulus of 227 GPa. Additionally, as a filler, potassium titanate

whisker (PTW) friction material was introduced. PTW is a fiber-like substance which possess excellent physical and mechanical properties with tensile strength of 6.68 GPa and tensile modulus of 274.4 GPa [20]. Addition of PTW into a polymer matrix improves abrasion, skid resistance and dimension stability. General formula of PTW is $K_2O$. $nTiO_2$ where n is a variable. Based on molar ratio of $TiO_2$ content to $K_2O$ content, PTW are generally classified as monotitanate (n=1), hexatitanate (n=6) and octatitanate (n=8). In this work, hexatitanate was used. The physical and thermal characteristics of these composite constituents are provided in Table 1 for reference.

**Table 1.** Properties of composite's constituents.

| Parameters | PES | SCF | PTW |
|---|---|---|---|
| Density (g/cm$^3$) | 1.37 | 1.80 | 3.13 |
| Melting temperature ($^o$C) | 330 | 3500 | 1300 |
| Thermal conductivity (W/m $^o$C) | 0.17 | 5.9 | 1.74 |
| Specific heat (J/g $^o$C) | 1.44 | 0.69 | 0.92 |
| Length (µm) | - | 900 | 10 |
| Diameter (µm) | - | 6 | 0.5 |
| Aspect ratio | - | 150 | 20 |
| Supplier | Solvay (USA) | Teijin (Japan) | Nobel Alchem (India) |
| Commercial name | Veradel [22] | Tenax [23] | TiNO-F [24] |

## 2.2 Fabrication

In a prior study from the same authors, it was determined that PES containing 30 wt.% of SCF exhibited the optimal mechanical characteristics [21]. For the mechanically optimized PES/SCF composite, it was planned to add the PTW filler such that total wt.% of fiber and filler should not exceed 30 wt.%. Hence SCF content was limited to 25 wt.% and PTW to 5 wt.%.

PES and 25 wt. % of SCFs was melt mixed and compounded along with the filler as per the formulations shown in Table 2, in ZE 40 twin screw extruder (Make: KraussMaffei Berstorff) operated at a screw speed of 500 rpm with an output rate 40 kg/hour. The extruder barrel with 11 stages was maintained at temperatures of 350-350-340-340-340-330-330-330-330-340-350 °C along its length from hopper (feed) to die (output) side. Compounded material extruding out of the die (ϕ 3 mm) was cooled by taking through water bath and then chopped for a length of 2.5 mm using a pelletizer. These pellets from the twin-screw extruder were preheated at 110 °C for 2 hours to eliminate moisture content. The preheated pellets were then fed into a Milacron Nova Servo 80T injection molding machine. The molding process settings were configured according to the parameters outlined in Table 3.

**Table 2.** Material formulations and designations.

| Composites | Matrix wt. %, PES | Fiber wt. %, SCF | Filler wt. %, PTW |
|---|---|---|---|
| $C_{00}P$ | 100 | 00 | - |
| $C_{25}P$ | 75.0 | 25 | - |
| $C_{25}W_{2.5}P$ | 72.5 | 25 | 2.5 |
| $C_{25}W_{5.0}P$ | 70.0 | 25 | 5.0 |

**Table 3.** Injection moulding parameters.

| Temperature along the barrel (°C) | | | | Injection Speed (mm/s) | Injection Pressure (bar) | Screw Speed (rpm) |
|---|---|---|---|---|---|---|
| Zone 1 | Zone 2 | Zone 3 | Nozzle | | | |
| 320 | 325 | 335 | 345 | 110 | 140 | 100 |

**Fig. 1.** Pins cut from Injection moulded discs.

The molten material from the machine's nozzle was injected into a mold maintained at a constant temperature of 140 °C, under a pressure of 140 bar, for a duration of 3 seconds. Following this, the injection process continued at 60 bar for 6 seconds, succeeded by cooling for 20 seconds under atmospheric pressure. Upon ejection from the molds, specimens in the form of 100 mm diameter discs with a thickness of 3.85 mm were obtained. Additionally, rectangular cross-section samples (10 mm x 3.85 mm) measuring 125 mm in length were also molded. The injection procedure adhered to the guidelines established in the ISO 294 standard. To facilitate wear testing, a section of the molded disc was cut into an 8 mm diameter using water jet machining, as depicted in Fig. 1. This modified specimen was used for the conduction of wear test.

### 2.3 Characterization methods

Injection moulded strips of 125 mm length were cut into 10 small samples along its length as depicted in Fig. 2(b). Density and Barcol hardness of each small sample was measured as per ASTM D792 [25] and ASTM D2583 standard [26] standards respectively. This was done to ensure uniform dispersion of fibers and fillers in the matrix phase. Average density and hardness values of all the samples were reported as density and hardness of the respective composite. In the present tribological study, central composite design (CCD) which is a response surface method (RSM) based design of experiment (DOE) was used to formulate the number of experiments to analyze the wear resistance of PES/SCF composites.


**Fig. 2.** (a) Densometer (b) Samples for density and hardness test.

Experiments were designed by considering the load and speed as continuous factors with three levels in each and composites as categorized factor with four levels. Based on *pv* limit consideration, levels for normal load factor were selected as 4.9 N (0.5 kg), 9.8 N (1 kg) and 14.7 N (1.5 kg) and then levels of sliding velocity factor were selected as 1, 2 and 3 m/s. Minimum, mean and maximum levels of continuous factors are presented in Table 4. This resulted in 13x4=52 experiment runs as detailed in Table 5. Sliding distance (3000 m) was taken as fixed for all the experiments. Track diameter was fixed to 90 mm for all the experiments except for those with speed of 0.6 m/s. A two-body sliding wear test was carried out following ASTM G99 [27] guidelines, utilizing a 200 N capacity tribometer depicted in Fig. 3 (Manufactured by Ducom, TR-20 model). A circular specimen with an 8 mm diameter and a height of 3.85 mm, as shown in Fig. 1, was affixed to a specially designed pin. This pin was then pressed against a steel disc possessing a hardness of 35HRC. To ensure uniformity, all composite specimens underwent pre-wearing by rubbing against #1200 sandpaper. Subsequently, the specimens were subjected to a 15-minute ultrasonic cleaning in ethanol.

**Fig. 3.** Pin-on-disc tribometer.

**Table 4.** Continuous factors and their levels.

| Factors | Levels | | |
|---|---|---|---|
| | Min (-1) | Mean (0) | Max (+1) |
| Load, P (N) | 4.9 | 9.8 | 14.7 |
| Speed, v (m/s) | 1 | 2 | 3 |

**Table 5.** Experiment run orders.

| Factors | | | | | |
|---|---|---|---|---|---|
| Load, P (N) | Speed, v (m/s) | Composites, C | | | |
| | | $C_{00}P$ | $C_{25}P$ | $C_{25}W_{2.5}P$ | $C_{25}W_{5.0}P$ |
| | | Experiment Run orders | | | |
| 4.9 | 1 | 19 | 49 | 23 | 16 |
| 14.7 | 1 | 1 | 13 | 10 | 2 |
| 4.9 | 3 | 6 | 30 | 21 | 5 |
| 14.7 | 3 | 3 | 22 | 17 | 20 |
| 2.9 | 2 | 34 | 45 | 15 | 9 |
| 16.7 | 2 | 18 | 27 | 43 | 28 |
| 9.8 | 0.6 | 36 | 42 | 25 | 35 |
| 9.8 | 3.4 | 4 | 33 | 24 | 47 |
| 9.8 | 2 | 8 | 37 | 11 | 44 |
| 9.8 | 2 | 46 | 52 | 41 | 31 |
| 9.8 | 2 | 39 | 38 | 29 | 7 |
| 9.8 | 2 | 50 | 40 | 48 | 12 |
| 9.8 | 2 | 32 | 51 | 26 | 14 |

The surface roughness of the cleaned specimens was quantified using a roughness tester (Manufactured by Metrix+, Microsurf 10 A). The measured arithmetic mean roughness ($R_a$) and linear distance between the peak and valley ($R_Z$) values for the pre-worn composites ranged between 0.4-0.8 μm and 1.0-2.0 μm, respectively. Notably, the mold-finished surfaces of the composites exhibited $R_a$ and $R_z$ values in the range of 0.1-8.0 μm and 0.2-23 μm, respectively, with composites featuring mold surface finish showing higher $R_z$ values, indicating greater unevenness.

## 3. RESULTS AND DISCUSSION

### 3.1 Density and hardness tests

All the ten cut samples of each composite showed density and hardness values with ±1% variation with their means as indicated in Table 6. This signified the uniform dispersion of fibers/fillers in the PES matrix phase.

**Table 6.** Physical properties of PES/SCF composites.

| Composites | Density (g/cm³) | Hardness (Barcol) |
|---|---|---|
| $C_{00}P$ | 1.364 | 34 |
| $C_{25}P$ | 1.412 | 49 |
| $C_{25}W_{2.5}P$ | 1.452 | 50 |
| $C_{25}W_{5.0}P$ | 1.461 | 51 |

Density of $C_{25}P$ composite increased by 3.52% with reference to neat PES due to 25 wt.% of SCF reinforcement. Furthermore, densities were increased by 2.83% and 3.47% due to the addition of PTW filers by 2.5 wt.% and 5 wt.% respectively in $C_{25}P$ composite. Increased densities were due to higher density of PTW than PES and SCFs. Average hardness and density values of the PES/SCF composites were presented in Table 6. In terms of Barcol scale, hardness of $C_{25}P$ composite increased by 44.1% due to the addition of 25 wt.% of SCFs into neat PES. In the case of 2.5 and 5 wt.% of PTW filled composites, marginal improvement in hardness by 2.04% and 4.08% was observed respectively with respect to $C_{25}P$ unfilled composite. Enhancement in the hardness of PTW filled composites was due to the dispersion of harder PTW particles in the PES/SCF phase. Addition of whiskers increases the cross-link density of PES polymer chain due to which increase in hardness of PTW filled composites increases [11].

### 3.2 Wear test

Effect of PTW fillers on the tribological behaviour of PES/SCF composites were studied using CCD-RSM approach. Based on CCD-RSM matrix, 52 wear tests were conducted in the run order shown in Table 7. Three output responses were observed during the wear tests namely SWR, COF and contact bulk temperature $T_b$; and are provided in the Table 7.

### 3.3 Effects of tribological parameters on COF, SWR and $T_b$

As seen in main effect plots shown in Fig. 4(a)-(c), all the three factors P, v and C have influenced the COF, SWR and $T_b$ of the filled PES/SCF composites significantly. As reported in ANOVA Table 8, COF of the filled composites were mainly influenced due to the linear effect of composites (C) followed by quadratic effects of normal load (P) and sliding velocity ($v$). On the other hand, SWR of the filled composites were mainly influenced due to the linear effect of the composites (C) followed by linear effect of sliding velocity ($v$) as given in Table 9.

As friction is associated with conversion of mechanical energy into heat, the thermal state of friction contact decides the tribological behaviour of polymer composites. When the normal load was varied from 4.9 N to 9.8 N, the rise in bulk contact temperature between polymer pin and steel disc was observed around 30 °C and composite samples were operated at stabilized bulk temperature of around 70°C during the sliding test. However, local or film temperature at the contact asperities will be much higher than the bulk temperature which was estimated around 120 °C. This film temperature at the asperities between pin and disc was much less than glass transition temperature of PES polymer (220 °C) and hence asperities of polymer matrix did not soften and maintained its thermal stability during the sliding action without any sticking phenomenon. This indicated that temperature rise had negligible effect on frictional behaviour of polymer composites and according to the classical frictional theories, coefficient of friction decreased with increase in normal load. On the other hand, when the normal load was increased from 9.8 N to 14.9 N, bulk contact temperature raised to around 110 °C and resulted in film or local temperature of around 220 °C at the contact asperities. This made the polymer phase at contact asperities to transit from rigid state to rubbery state and sticking of the polymer phase on the sliding surface was observed. Due to the plasticizing of polymer phase on to the sliding surface, frictional force increased and resulted in increase in coefficient of friction and wear, indicating the strong influence of contact temperature on frictional behaviour of polymer composites [14].

**Table 7.** Experimental COF, SWR and $T_b$ of filled PES/SCF composites

| Std. Order | Run Order | Factors | | | COF | SWR x10$^{-6}$ mm$^3$/N-m | $T_b$ ($^o$C) |
|---|---|---|---|---|---|---|---|
| | | Load, P (N) | Velocity, *v* (m/s) | Composites C | | | |
| 2 | 1 | 14.7 | 1 | $C_{00}P$ | 0.336 | 60.6 | 62.4 |
| 41 | 2 | 14.7 | 1 | $C_{25}W_{5.0}P$ | 0.406 | 3.2 | 63.2 |
| 4 | 3 | 14.7 | 3 | $C_{00}P$ | 0.375 | 133.8 | 148.2 |
| 8 | 4 | 9.8 | 3.4 | $C_{00}P$ | 0.367 | 156.9 | 115.2 |
| 42 | 5 | 4.9 | 3 | $C_{25}W_{5.0}P$ | 0.382 | 19.5 | 58.1 |
| 3 | 6 | 4.9 | 3 | $C_{00}P$ | 0.355 | 164.6 | 63.5 |
| 50 | 7 | 9.8 | 2 | $C_{25}W_{5.0}P$ | 0.396 | 12.3 | 72.8 |
| 9 | 8 | 9.8 | 2 | $C_{00}P$ | 0.314 | 105.9 | 71.3 |
| 44 | 9 | 2.9 | 2 | $C_{25}W_{5.0}P$ | 0.408 | 22.8 | 38.6 |
| 28 | 10 | 14.7 | 1 | $C_{25}W_{2.5}P$ | 0.372 | 3.8 | 58.2 |
| 35 | 11 | 9.8 | 2 | $C_{25}W_{2.5}P$ | 0.354 | 13.4 | 68.9 |
| 51 | 12 | 9.8 | 2 | $C_{25}W_{5.0}P$ | 0.392 | 10.8 | 72.5 |
| 15 | 13 | 14.7 | 1 | $C_{25}P$ | 0.296 | 4.6 | 55.6 |
| 52 | 14 | 9.8 | 2 | $C_{25}W_{5.0}P$ | 0.394 | 12.3 | 73.4 |
| 31 | 15 | 2.9 | 2 | $C_{25}W_{2.5}P$ | 0.364 | 25.8 | 35.8 |
| 40 | 16 | 4.9 | 1 | $C_{25}W_{5.0}P$ | 0.414 | 12.3 | 33.8 |
| 30 | 17 | 14.7 | 3 | $C_{25}W_{2.5}P$ | 0.393 | 29.1 | 131.3 |
| 6 | 18 | 16.7 | 2 | $C_{00}P$ | 0.378 | 103.6 | 121.5 |
| 1 | 19 | 4.9 | 1 | $C_{00}P$ | 0.341 | 77.2 | 36.4 |
| 43 | 20 | 14.7 | 3 | $C_{25}W_{5.0}P$ | 0.438 | 25.6 | 155.3 |
| 29 | 21 | 4.9 | 3 | $C_{25}W_{2.5}P$ | 0.356 | 22.1 | 55.8 |
| 17 | 22 | 14.7 | 3 | $C_{25}P$ | 0.312 | 34.4 | 121.6 |
| 27 | 23 | 4.9 | 1 | $C_{25}W_{2.5}P$ | 0.379 | 14.0 | 32.4 |
| 34 | 24 | 9.8 | 3.4 | $C_{25}W_{2.5}P$ | 0.361 | 7.6 | 102.4 |
| 33 | 25 | 9.8 | 0.6 | $C_{25}W_{2.5}P$ | 0.385 | 7.6 | 32.9 |
| 39 | 26 | 9.8 | 2 | $C_{25}W_{2.5}P$ | 0.355 | 14.0 | 67.4 |
| 19 | 27 | 16.7 | 2 | $C_{25}P$ | 0.325 | 30.2 | 98.5 |
| 45 | 28 | 16.7 | 2 | $C_{25}W_{5.0}P$ | 0.426 | 22.5 | 116.6 |
| 37 | 29 | 9.8 | 2 | $C_{25}W_{2.5}P$ | 0.355 | 14.0 | 68.2 |
| 16 | 30 | 4.9 | 3 | $C_{25}P$ | 0.286 | 26.1 | 52.2 |
| 49 | 31 | 9.8 | 2 | $C_{25}W_{5.0}P$ | 0.391 | 12.8 | 73.1 |
| 13 | 32 | 9.8 | 2 | $C_{00}P$ | 0.316 | 107.1 | 69.5 |
| 21 | 33 | 9.8 | 3.4 | $C_{25}P$ | 0.305 | 28.2 | 92.8 |
| 5 | 34 | 2.9 | 2 | $C_{00}P$ | 0.337 | 116.9 | 37.3 |
| 46 | 35 | 9.8 | 0.6 | $C_{25}W_{5.0}P$ | 0.422 | 6.7 | 37.2 |
| 7 | 36 | 9.8 | 0.6 | $C_{00}P$ | 0.344 | 47.3 | 40.2 |
| 22 | 37 | 9.8 | 2 | $C_{25}P$ | 0.27 | 15.8 | 61.4 |
| 24 | 38 | 9.8 | 2 | $C_{25}P$ | 0.272 | 16.5 | 61.5 |
| 11 | 39 | 9.8 | 2 | $C_{00}P$ | 0.318 | 109.6 | 69.8 |
| 25 | 40 | 9.8 | 2 | $C_{25}P$ | 0.274 | 14.4 | 60.8 |
| 36 | 41 | 9.8 | 2 | $C_{25}W_{2.5}P$ | 0.352 | 14.5 | 67.5 |
| 20 | 42 | 9.8 | 0.6 | $C_{25}P$ | 0.292 | 11.0 | 30.6 |
| 32 | 43 | 16.7 | 2 | $C_{25}W_{2.5}P$ | 0.378 | 25.6 | 108.5 |
| 48 | 44 | 9.8 | 2 | $C_{25}W_{5.0}P$ | 0.395 | 11.8 | 72.4 |
| 18 | 45 | 2.9 | 2 | $C_{25}P$ | 0.298 | 30.5 | 32.7 |
| 10 | 46 | 9.8 | 2 | $C_{00}P$ | 0.315 | 103.4 | 70.5 |
| 47 | 47 | 9.8 | 3.4 | $C_{25}W_{5.0}P$ | 0.371 | 6.7 | 108.4 |
| 38 | 48 | 9.8 | 2 | $C_{25}W_{2.5}P$ | 0.351 | 12.2 | 69.1 |
| 14 | 49 | 4.9 | 1 | $C_{25}P$ | 0.304 | 16.5 | 35.8 |
| 12 | 50 | 9.8 | 2 | $C_{00}P$ | 0.313 | 104.6 | 70.9 |
| 26 | 51 | 9.8 | 2 | $C_{25}P$ | 0.271 | 16.5 | 61.2 |
| 23 | 52 | 9.8 | 2 | $C_{25}P$ | 0.268 | 17.2 | 60.6 |

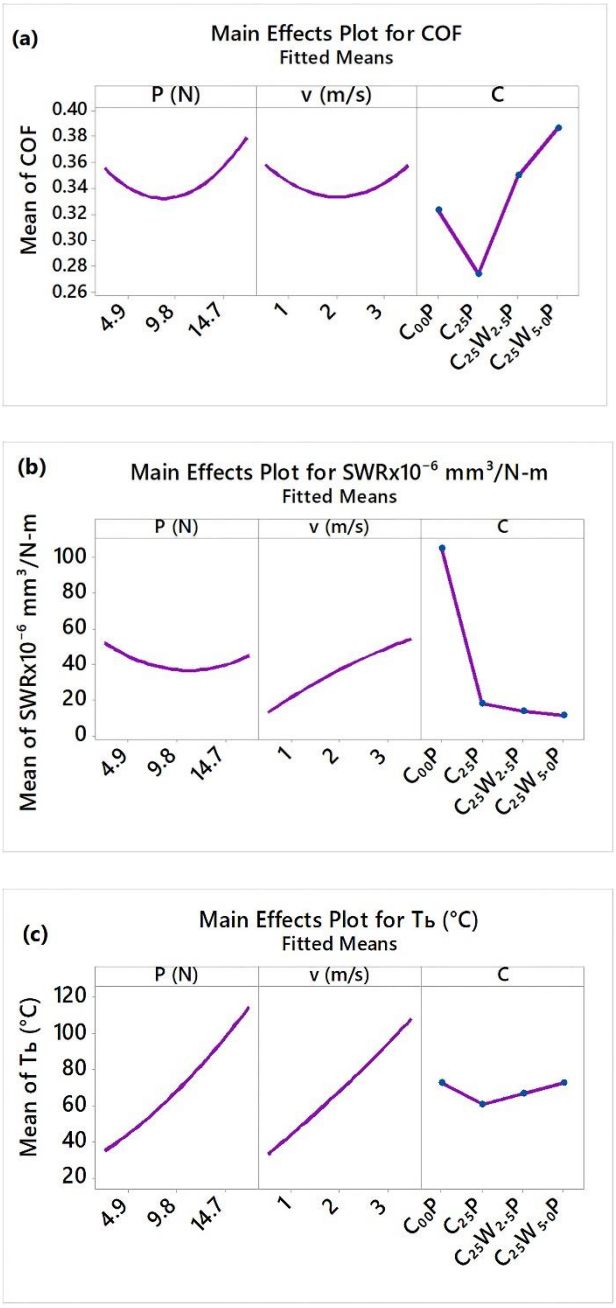


**Fig. 4.** Main effect plots of (a) COF (b) SWR (c) $T_b$ of filled composites.

Furthermore, $T_b$ response of the filled composites was strongly influenced due to the linear effect of load, velocity and composites sequentially as seen in Table 10. COF of PTW filled hybrid composites were affected strongly due to the addition of fillers to the larger extent than the SWR of PES/SCF composites as seen in Fig. 4(a)-(b).

### 3.4 Effect of filler reinforcement

Neat PES exhibited a mean of COF of 0.320 as seen Fig. 4(a). With addition of 25 wt.% of SCF, mean of COF decreased by 15.6%. Due to the pulverization of SCFs during sliding action, lubricative transfer film containing graphite particles is formed and resulted in reduction of COF [7]. Increase in mean COF was observed with the addition of PTW filler. COF values of PTW filled composites were observed higher than that of neat PES. As PTW is inorganic filler, it increases the abrasive force during the friction process and hence COF increased with the addition of PTW [28]. In addition, debris of PTW formed on the disc surface creates three body abrasive interactions [13]. Enhancement in the COF may also be associated with the titanium elements present in potassium titanate whiskers. Furthermore, SWR of PTW filled composites decreased with respect to the $C_{25}P$ composite. This could be attributed to the improvement in hardness and compressive modulus of the PTW filled composites. Since a specimen is loaded under compression in the pin-on-disk test, the tribological process is influenced mainly by the compression properties of the materials. The results reveal that the wear of the materials decreases markedly with increasing compression modulus. While a higher stiffness reduces the real contact surface, which leads to a lower adhesion, it results in a higher resistance force in the sliding direction, which leads to higher friction.

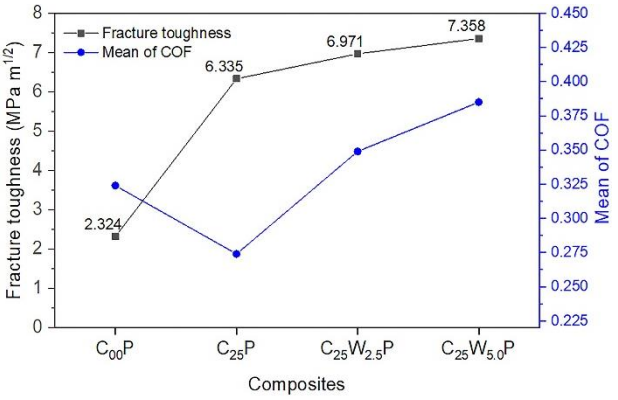


**Fig. 5.** Mean COF versus fracture toughness of filled PES/SCF composites.

Though improvement in the fracture toughness of PTW filled PES/SCF composites were noticed, their COF values were not decreased due to the presence of titanium elements as identified by EDX analysis which offers higher COF against the steel disc. However, wear resistance of the PTW filled composites increased which may be linked to their improvement in fracture toughness values. Furthermore, temperature

measurements revealed that 5 wt.% of PTW filled PES/SCF composite (Fig. 7(b)) showed maximum $T_b$ of 155.3 °C at (14.7 N, 3 m/s) which is higher than that of neat PES due to increase in the COF; however, PTW filled composites were stable due to improved thermal conductivity [29].

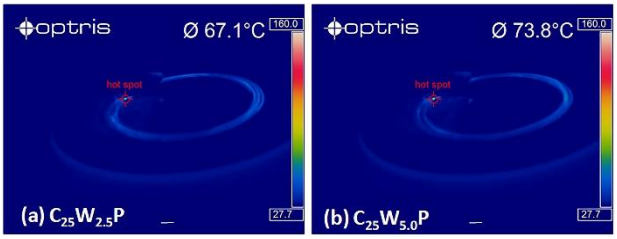


**Fig. 6.** Typical infrared images at steady state wear period at 9.8 N and 2 m/s.

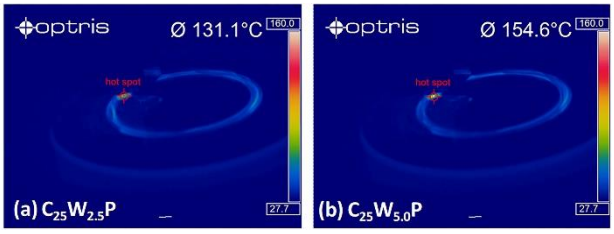


**Fig. 7.** IR images of PTW filled composites under 14.7 N and 3 m/s.

### 3.5 Effect of normal load

Decreasing trend in mean COF and mean SWR was noticed initially in PTW filled composites with the increase in normal load. This trend may be associated with the generated heat favoring the sliding process and forming the stable counter film. Above the load of 9.8 N and 2 m/s velocity, frictional heating dominates the wear process and leads to the thermal softening of the composites. Hence, higher COF and SWR were observed in PTW filled composites above the applied normal load of 9.8 N. In summary, maximum safe load at which minimum COF and SWR exhibited by filled composites was slightly lower than 9.8 N. However, it is possible to operate the composites safely at higher load of 14.7 N by decreasing the sliding velocity to 0.5 m/s.

### 3.6 Effect of sliding velocity

Mean COF of PTW filled composites decreased initially with the sliding velocity under the constant mean load. In contrast, mean SWR of filled PES/SCF composites tend to increase with the sliding velocity. This can be accounted for the continuous increase in the temperature due to the increase in sliding velocity. However, an insignificant increase in the mean SWR was noticed in the filled composites above 2 m/s. It is worth to note that surface melting due to frictional heating occurs easily at an engineering velocity in the case of typical semicrystalline polymers and much high wear rate appears when the sliding velocity exceeds a certain critical value which depends upon the type of polymer [30]. Fig. 7 shows IR images of 2.5 and 5 wt.% of PTW filled composites tested with 14.7 N normal load and 3 m/s sliding velocity. At 9.8 N load and 2 m/s velocity, 2.5 and 5 wt.% of PTW filled composites showed steady state temperature of 67.1 °C and 73.8 °C respectively as noticed in Fig. 6. However, due to increase in both load and velocity, contact temperature found to drastically increase to 131.1 °C and 154.6 °C in the PTW filled composites. This was mainly due to the higher COF acquired by the PTW filled composites. In addition, the sliding track was observed at elevated temperature and few patches formed on the disc due to the adhesion of PTW and SCFs. This indicates the domination of adhesive mode of wear above 2 m/s and hence, SWR of the PTW filled composites increased when sliding was made above 2 m/s. At moderate interface bulk temperature range (60-80 °C), local surface heating takes place and results in the reduction of shear stress. However, the subsurface deformation characteristics of the composites remain unaffected and asperity contact area remains same. Hence, COF of the composites decreases when they slide with moderate bulk temperature. On the other hand, when composites slide with higher interface bulk temperature (80-150 °C), subsurface softening occurs due to which contact area increases. This leads to the increase in COF. When bulk temperature goes above 150 °C, frictional force and COF increases rapidly due to the growth of the asperity contact junction.

In conclusion, only minor variation in the specific wear rate was noticed due to the addition of filler. However, the added filler showed significant variations in COF values of the filled composites. Furthermore, higher values of *pv* (pressure x velocity) resulted in higher specific wear rate in the filled composites.

**Table 8.** ANOVA results of COF of filled PES/SCF composites.

| Source | DF | Adj SS | Adj MS | F-Value | P-Value | Remarks |
|---|---|---|---|---|---|---|
| Model | 14 | 0.101599 | 0.007257 | 87.46 | 0.000 | Significant |
| Linear | 5 | 0.089274 | 0.017855 | 215.18 | 0.000 | Significant |
| P (N) | 1 | 0.001991 | 0.001991 | 24.00 | 0.000 | Significant |
| *v* (m/s) | 1 | 0.000001 | 0.000001 | 0.01 | 0.906 | Insignificant |
| C | 3 | 0.087282 | 0.029094 | 350.63 | 0.000 | Significant |
| Square | 2 | 0.008769 | 0.004385 | 52.84 | 0.000 | Significant |
| P x P | 1 | 0.006450 | 0.006450 | 77.73 | 0.000 | Significant |
| *v* x *v* | 1 | 0.003390 | 0.003390 | 40.85 | 0.000 | Significant |
| 2-Way Interaction | 7 | 0.003555 | 0.000508 | 6.12 | 0.000 | Significant |
| P x *v* | 1 | 0.001743 | 0.001743 | 21.01 | 0.000 | Significant |
| P x C | 3 | 0.000054 | 0.000018 | 0.22 | 0.885 | Insignificant |
| *v* x C | 3 | 0.001758 | 0.000586 | 7.06 | 0.001 | Significant |
| Error | 37 | 0.003070 | 0.000083 | | | |
| Lack-of-Fit | 21 | 0.003005 | 0.000143 | 35.11 | 0.000 | Significant |
| Pure Error | 16 | 0.000065 | 0.000004 | | | |
| Total | 51 | 0.104669 | | | | |

Model Summary and regression equations of COF:

| S | R-sq | R-sq(adj) | R-sq(pred) |
|---|---|---|---|
| 0.0091091 | 97.07% | 95.96% | 92.89% |

| | |
|---|---|
| $C_{00}P$ | $COF = 0.4302 - 0.01483\,P - 0.05433\,v + 0.000634\,P^2 + 0.01104\,v^2 + 0.002130\,P\,v$ |
| $C_{25}P$ | $COF = 0.4027 - 0.01526\,P - 0.06298\,v + 0.000634\,P^2 + 0.01104\,v^2 + 0.002130\,P\,v$ |
| $C_{25}W_{2.5}P$ | $COF = 0.4929 - 0.01542\,P - 0.06952\,v + 0.000634\,P^2 + 0.01104\,v^2 + 0.002130\,P\,v$ |
| $C_{25}W_{5.0}P$ | $COF = 0.5330 - 0.01481\,P - 0.07404\,v + 0.000634\,P^2 + 0.01104\,v^2 + 0.002130\,P\,v$ |

**Table 9.** ANOVA results of SWR x $10^{-6}$ of filled PES/SCF composites.

| Source | DF | Adj SS | Adj MS | F-Value | P-Value | Remarks |
|---|---|---|---|---|---|---|
| Model | 14 | 94894.8 | 6778.2 | 322.52 | 0.000 | Significant |
| Linear | 5 | 86481.0 | 17296.2 | 822.99 | 0.000 | Significant |
| P (N) | 1 | 186.4 | 186.4 | 8.87 | 0.005 | Significant |
| *v* (m/s) | 1 | 6117.6 | 6117.6 | 291.09 | 0.000 | Significant |
| C | 3 | 80177.0 | 26725.7 | 1271.66 | 0.000 | Significant |
| Square | 2 | 861.0 | 430.5 | 20.48 | 0.000 | Significant |
| P x P | 1 | 725.7 | 725.7 | 34.53 | 0.000 | Significant |
| *v* x *v* | 1 | 64.3 | 64.3 | 3.06 | 0.088 | Insignificant |
| 2-Way Interaction | 7 | 7552.8 | 1079.0 | 51.34 | 0.000 | Significant |
| P x *v* | 1 | 92.2 | 92.2 | 4.39 | 0.043 | Significant |
| P x C | 3 | 367.6 | 122.5 | 5.83 | 0.002 | Significant |
| *v* x C | 3 | 7093.0 | 2364.3 | 112.50 | 0.000 | Significant |
| Error | 37 | 777.6 | 21.0 | | | |
| Lack-of-Fit | 21 | 744.8 | 35.5 | 17.28 | 0.000 | Significant |
| Pure Error | 16 | 32.8 | 2.1 | | | |
| Total | 51 | 95672.4 | | | | |

Model Summary and regression equation of SWR:

| S | R-sq | R-sq(adj) | R-sq(pred) |
|---|---|---|---|
| 4.58437 | 99.19% | 98.88% | 97.83% |

| | |
|---|---|
| $C_{00}P$ | $SWR = 66.46 - 6.839\,P + 40.74\,v + 0.2127\,P^2 - 1.521\,v^2 + 0.490\,P\,v$ |
| $C_{25}P$ | $SWR = 26.99 - 5.254\,P + 9.25\,v + 0.2127\,P^2 - 1.521\,v^2 + 0.490\,P\,v$ |
| $C_{25}W_{2.5}P$ | $SWR = 29.93 - 5.240\,P + 5.46\,v + 0.2127\,P^2 - 1.521\,v^2 + 0.490\,P\,v$ |
| $C_{25}W_{5.0}P$ | $SWR = 28.95 - 5.233\,P + 4.99\,v + 0.2127\,P^2 - 1.521\,v^2 + 0.490\,P\,v$ |

**Table 10.** ANOVA results of $T_b$ of filled PES/SCF composites.

| Source | DF | Adj SS | Adj MS | F-Value | P-Value | Remarks |
|---|---|---|---|---|---|---|
| Model | 14 | 47892.4 | 3420.9 | 519.65 | 0.000 | Significant |
| Linear | 5 | 44010.0 | 8802.0 | 1337.08 | 0.000 | Significant |
| P (N) | 1 | 22740.7 | 22740.7 | 3454.44 | 0.000 | Significant |
| *v* (m/s) | 1 | 20060.5 | 20060.5 | 3047.32 | 0.000 | Significant |
| C | 3 | 1208.8 | 402.9 | 61.21 | 0.000 | Significant |
| Square | 2 | 266.6 | 133.3 | 20.25 | 0.000 | Significant |
| P x P | 1 | 250.7 | 250.7 | 38.09 | 0.000 | Significant |
| *v* x *v* | 1 | 36.1 | 36.1 | 5.49 | 0.025 | Significant |
| 2-Way Interaction | 7 | 3615.8 | 516.5 | 78.47 | 0.000 | Significant |
| P x *v* | 1 | 3186.6 | 3186.6 | 484.06 | 0.000 | Significant |
| P x C | 3 | 234.6 | 78.2 | 11.88 | 0.000 | Significant |
| *v* x C | 3 | 194.6 | 64.9 | 9.85 | 0.000 | Significant |
| Error | 37 | 243.6 | 6.6 | | | |
| Lack-of-Fit | 21 | 237.6 | 11.3 | 30.38 | 0.000 | Significant |
| Pure Error | 16 | 6.0 | 0.4 | | | |
| Total | 51 | 48136.0 | | | | |

Model Summary and regression equations of $T_b$:

| S | R-sq | R-sq(adj) | R-sq(pred) |
|---|---|---|---|
| 2.56574 | 99.49% | 99.30% | 98.73% |

| | |
|---|---|
| $C_{00}P$ | $T_b = 33.41 - 2.349\,P - 5.41\,v + 0..1250\,P^2 + 1.139\,v^2 + 2.880\,P\,v$ |
| $C_{25}P$ | $T_b = 45.80 - 3.561\,P - 11.49\,v + 0..1250\,P^2 + 1.139\,v^2 + 2.880\,P\,v$ |
| $C_{25}W_{2\cdot5}P$ | $T_b = 39.85 - 3.004\,P - 8.43\,v + 0.1250\,P^2 + 1.139\,v^2 + 2.880\,P\,v$ |
| $C_{25}W_{5\cdot0}P$ | $T_b = 32.00 - 2.167\,P - 5.65\,v + 0.1250\,P^2 + 1.139\,v^2 + 2.880\,P\,v$ |

### 3.7 Response surface models for wear of filled PES/SCF composites

ANOVA checks the model adequacy and shows the level to which predicted values are accurate. ANOVA results for COF, SWR and $T_b$ of filled PES/SCF composites are provided in Table 8, Table 9 and Table 10 respectively. Based on RSM-CCD model, regression equations for the COF, SWR and $T_b$ of categorized filled PES/SCF composites were developed. Quadratic models of COF, SWR and $T_b$ of PTW filled composites showed F-test values of 87.46, 322.52 and 519.65 respectively with small probability values of 0.000. This indicates that developed regression model for the above three responses is highly dependent on all the factors used in the model. $R^2$ value illustrate the percentage of variability of predicted responses by the model. The value of $R^2$ for COF, SWR and $T_b$ were 97.07%, 99.19% and 99.49% respectively. As the value of $R^2$ is close to 1 in all the above responses, the developed quadratic model predicts the COF, SWR and $T_b$ of filled PES/SCF composites more precisely in the considered factors range or levels. Even though lack-of-fit is seen as statistically significant, it was mainly due to the small pure error value provided by the closer replicate response values of the independent variables in the model [31-32] and hence, model is fitted perfectly with the experimental values.

### 3.8 Validation of wear models of filled PES/SCF composites

Residuals of COF, SWR and $T_b$ of filled PES/SCF composites followed the straight line and hence they are normally distributed with slight scattering as shown in Fig. 8(a)-(c). As the residual data shows normal probability distribution, the developed regression model is considered as highly validated with the experimental observations. Furthermore, residuals (errors) of COF and SWR in the observation order are randomly distributed across the graph without any noticeable pattern and structure.

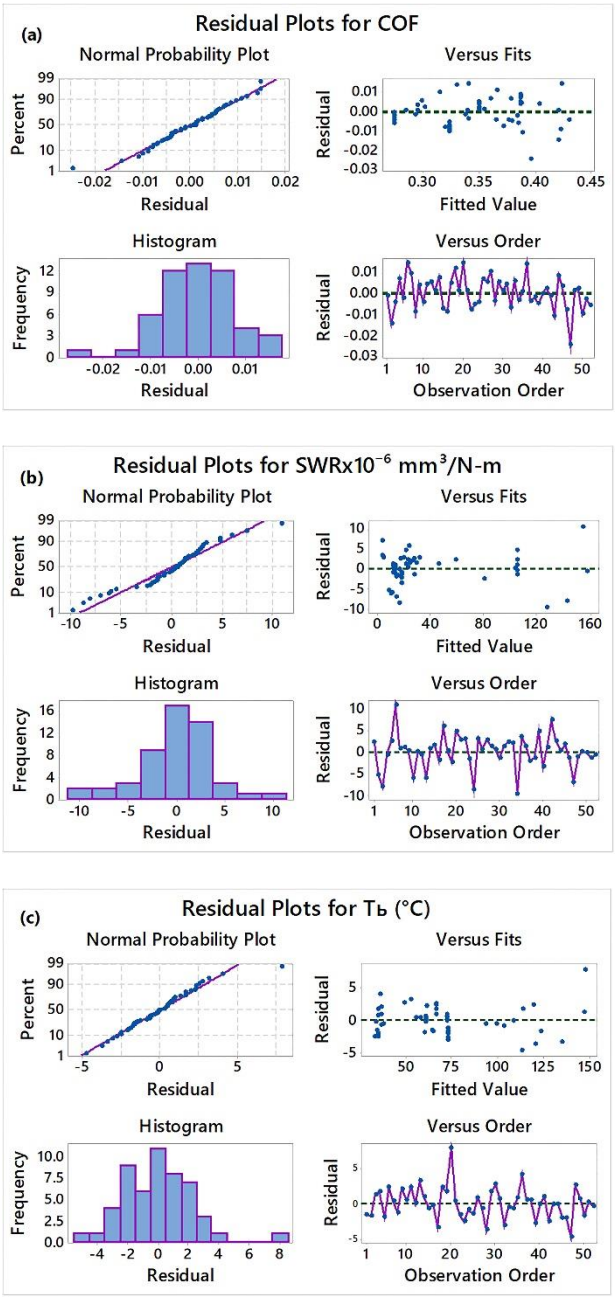


**Fig. 8.** Residual plots for (a) COF (b) SWR (c) $T_b$ of filled PES/SCF composites.

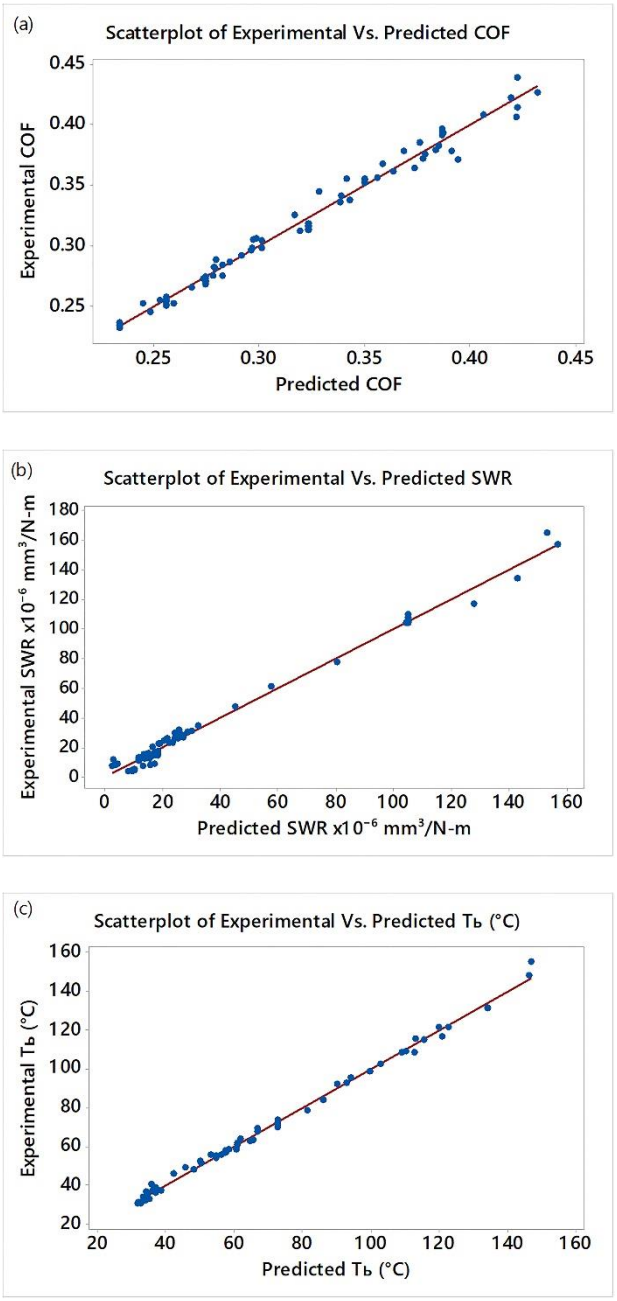


**Fig. 9.** Plot between predicted and experimental data of (a) COF (b) SWR (c) $T_b$.

This confirms that residuals are independent and normally distributed. Hence, the developed regression models are satisfactory and adequate. Plots of predicted versus experimental COF, SWR and $T_b$ of filled PES/SCF composites are presented in Fig. 9 (a)-(c). In COF, SWR and Tb plots, points are scattered along the diagonal line. Furthermore, diagonal line appears to be passing through origin which is the indication of small deviation between the experimental and predicted output responses.

### 3.9 Response surface analysis of filled PES/SCF composites

Contour and response surface plots of COF, SWR and $T_b$ responses of filled PES/SCF composites are presented in Fig. 10, Fig. 11 and Fig. 12 respectively. Interaction plots between the continuous factors P and *v*; and categorized factor C are given in Fig. 13(a) for COF response, Fig. 13(b) for SWR response and Fig. 13(c) for $T_b$ response. These plots indicate the actual amount of COF, SWR and $T_b$ at the coded levels low (-1), mean (0) and high (+1).

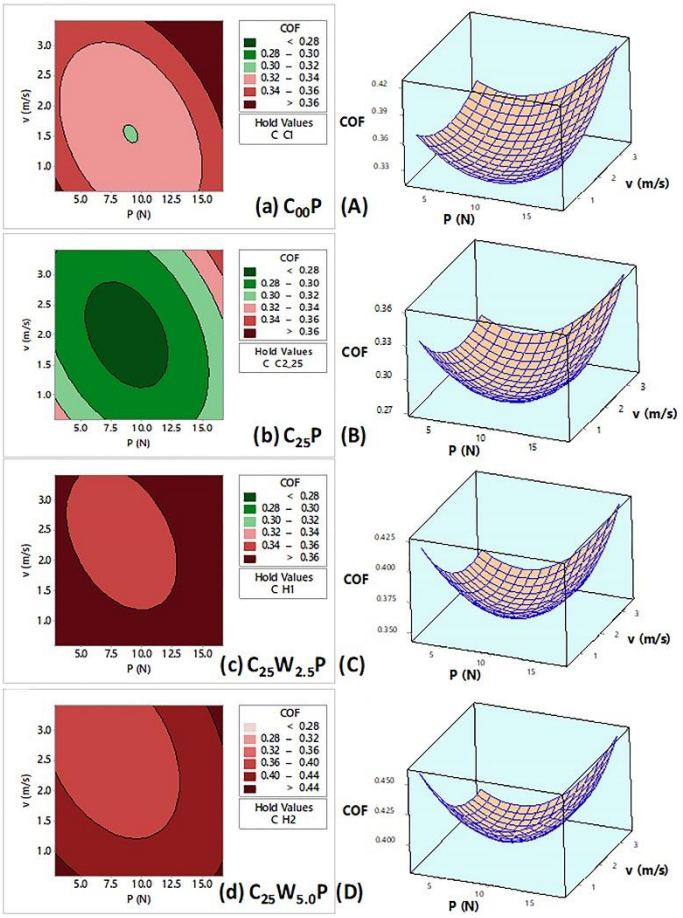


**Fig. 10.** Contour (a-f) and surface (A-F) plots of COF of filled composites.

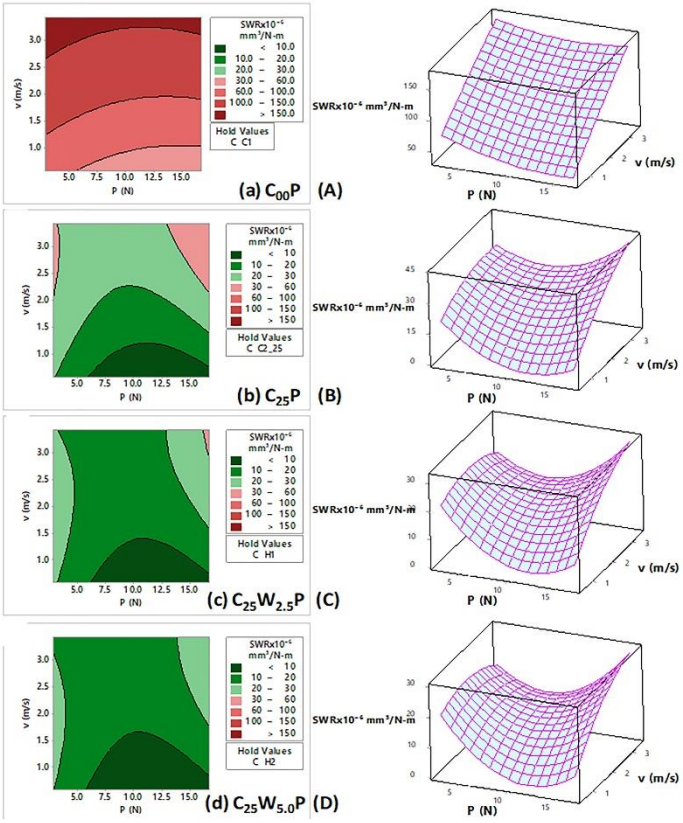


**Fig. 11.** Contour (a-f) and surface (A-F) plots of SWR of filled composites.

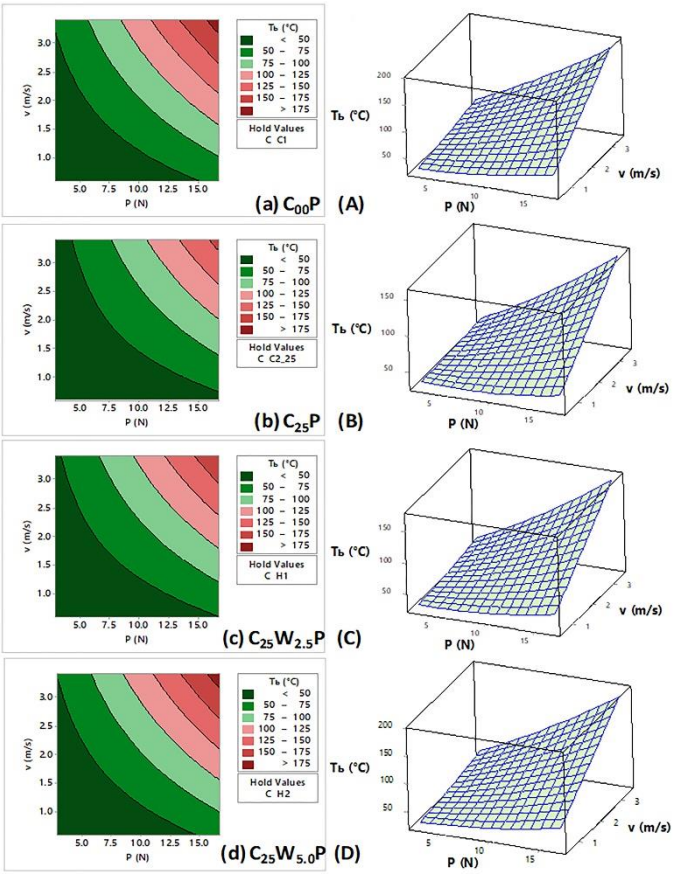


**Fig. 12.** Contour (a-f) and surface (A-F) plots of $T_b$ of filled composites.

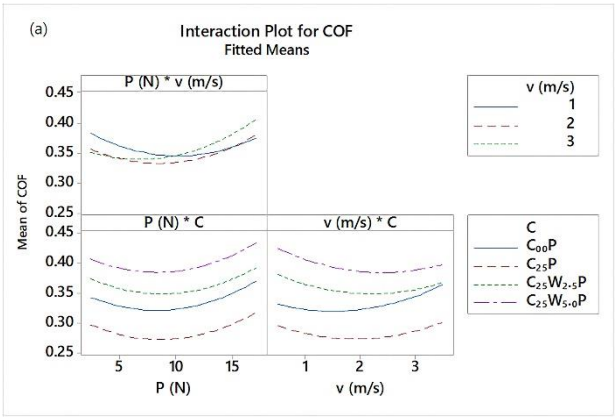


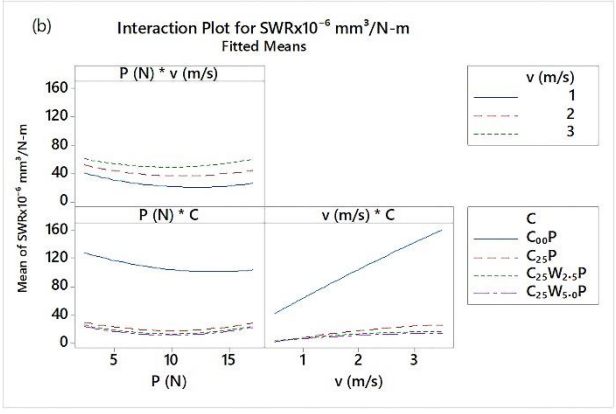


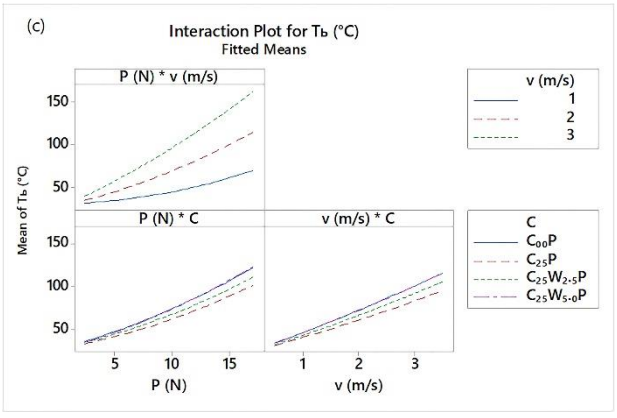


**Fig. 13.** Interaction plots for (a) COF (b) SWR (c) $T_b$ of filled composites.

In applications such as brake pads, developed composite material needs to be optimized for minimum SWR with maximum COF. This is the case of optimization problem where multiple objectives with opposite nature should be met at a time. As determined from response optimizer plot shown in Fig. 14, $C_{25}W_{5.0}P$ composite i.e. PES/SCF composite with 5 wt.% of PTW showed maximum COF of 0.438 and minimum 6.47 x $10^{-6}$ $mm^3$/N-m under the optimum operating conditions of 15.9 N load

and 0.58 m/s sliding velocity. In summary, PTW filled composites are the first choice for the tribo-applications which seek for high friction.

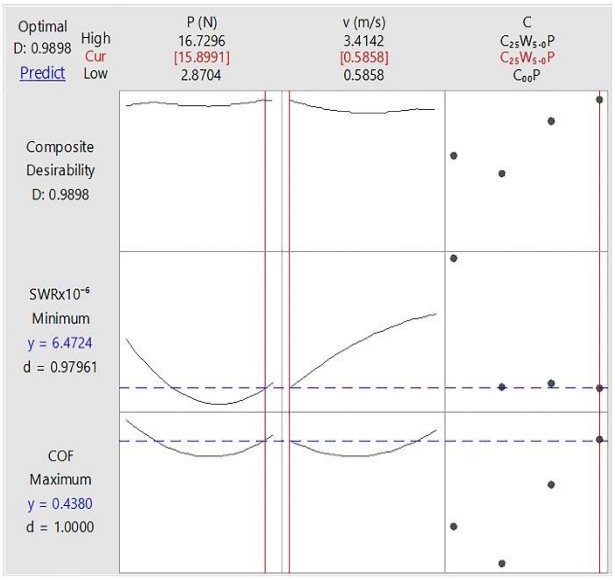


**Fig. 14.** Response optimizer plot of filled composites with maximum COF.

### 3.10 Validation of wear models for predicting COF, SWR and $T_b$

The developed response surface models of filled PES/SCF composites were validated by performing the supplementary wear tests on $C_{25}W_{5.0}P$ composite under a fixed sliding distance of 3000 m, fixed optimized sliding velocity of 1.4 m/s for different normal loads of 4.9 N, 9.8 N and 14.7 N. Supplementary wear test results i.e. COF, SWR and $T_b$ were compared with that of the predicted results from RSM model as reported in Table 11.

**Table 11.** Validation of regression model of $C_{25}W_{5.0}P$.

| Load (N) | Condition | COF | SWR×10$^{-6}$ mm$^3$/N-m | $T_b$ (°C) |
|---|---|---|---|---|
| 4.9 | Predicted | 0.408 | 15.77 | 38.5 |
| | Experimental | 0.411 | 15.83 | 39.7 |
| 9.8 | Predicted | 0.395 | 8.81 | 56.6 |
| | Experimental | 0.398 | 8.92 | 57.8 |
| 14.7 | Predicted | 0.414 | 12.06 | 80.7 |
| | Experimental | 0.418 | 12.14 | 81.4 |

Predicted data were found close to that of the experimental values. Hence, predicted modes of COF, SWR and $T_b$ responses of all the filled PES/SCF composites are accepted.

### 3.11 Morphology of worn surfaces of filled PES/SCF composites

SEM examinations were made on the worn surfaces of filled PES/SCF composites tested under lower, moderate and higher test conditions (P, *v*). At lower normal load and lower sliding velocity combinations (4.9 N, 1 m/s), worn surface of neat PES was found quite smooth as in Fig. 15 and could resist the abrasive wear and hence showed lower wear rate. However, with increase in sliding velocity, measured contact temperature significantly increased and lead to the severe wear as there was no support from the SCFs. At this test condition, PES was found to be at 40 °C.

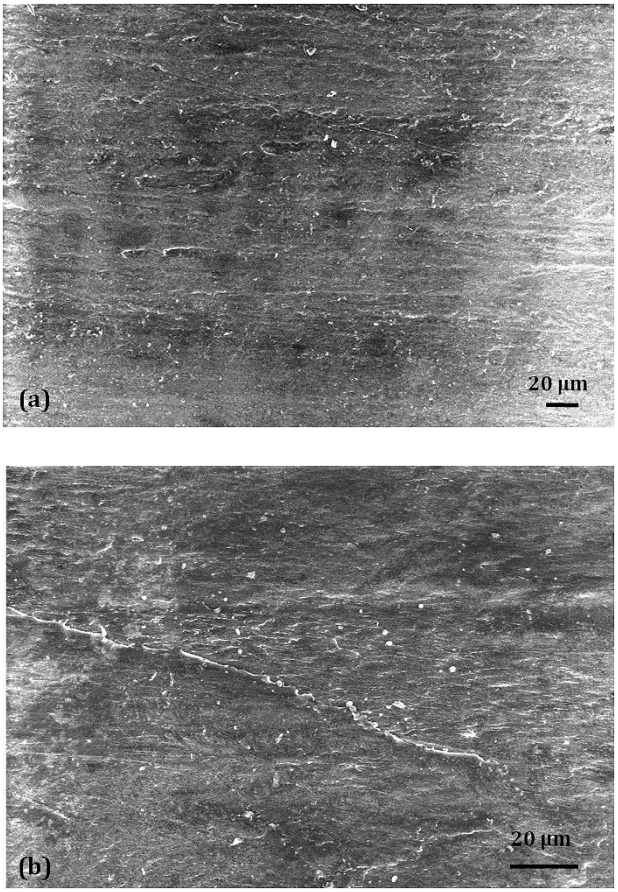


**Fig. 15.** Worn surfaces of neat PES at 4.9 N and 1 m/s (a) 500x (b) 1000x.

Worn surfaces of neat PES tested at 9.8 N and 2 m/s were reported in Fig. 16, wherein more ploughed, plucked and plasticized marks were observed with micro grooves. These grooves were formed in the direction of sliding due to the abrasive wear created by hard asperities present on the rotating disc.

As abrasive wear is more dangerous than adhesive type of wear in polymer composites, more material loss was noticed. Hence, severe abrasive wear was occurred in neat PES at direct asperity contact areas at medium loading conditions. Furthermore, wear debris produced during the sliding process were in the form of small particles, few of which were attaching to the counterface disc and few were flying out due to centrifugal effect. At this test conditions, average contact temperature was measured approximately 75 °C.

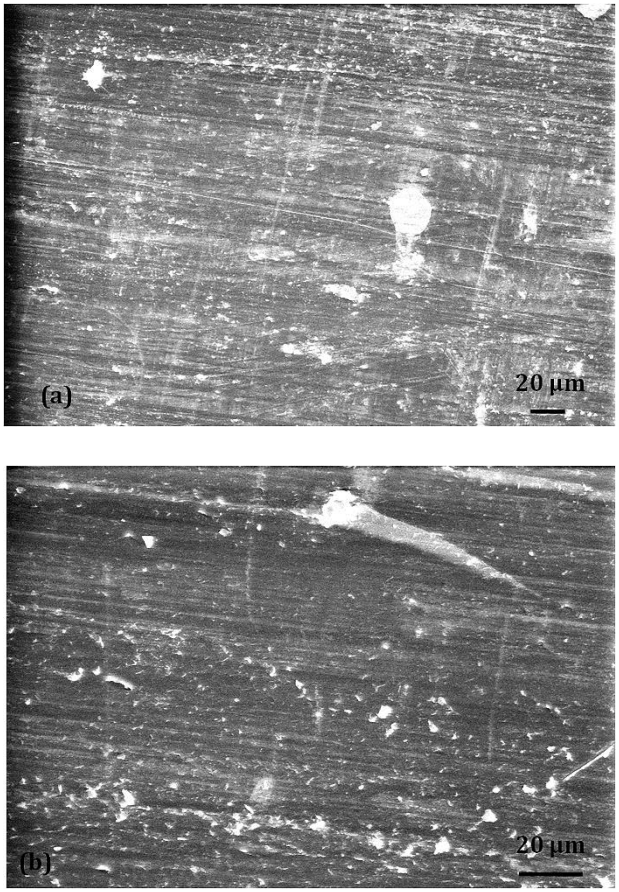


**Fig. 16.** Worn surfaces of neat PES at 9.8 N and 2 m/s (a) 500x (b) 1000x.

Furthermore, with higher normal load and higher sliding velocity, worn surfaces showed rough surfaces with melted and plasticized marks as in Fig. 17. In this case, measured bulk temperature was found around 150 °C, while estimated flash temperature was around 260 °C which is near to the $T_g$ of neat PES. This confirms that at higher loading conditions, higher interface temperature due to frictional heating melts the polymer at contact junctions and results in higher wear rate.

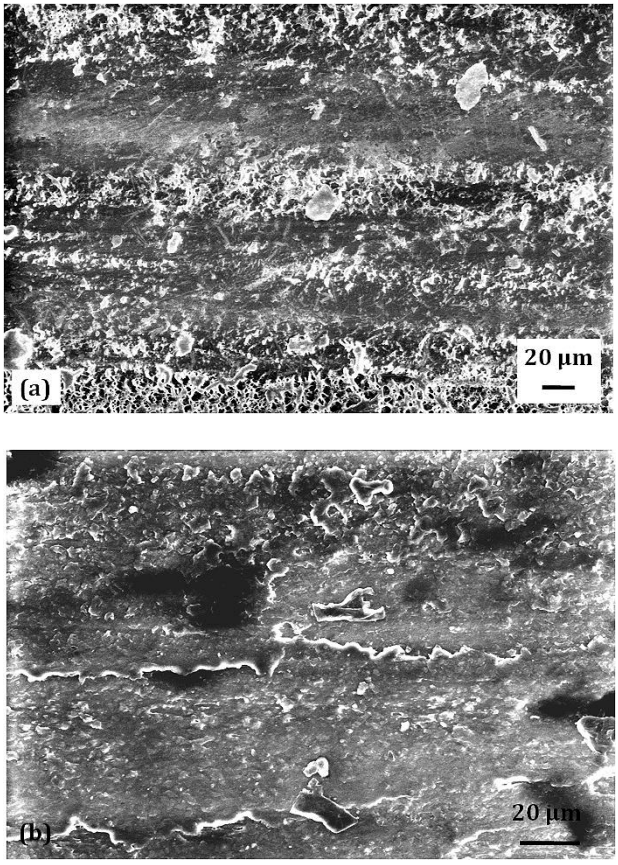


**Fig. 17.** Worn surfaces of PES at 14.7 N and 3 m/s (a) 500x (b) 1000x.

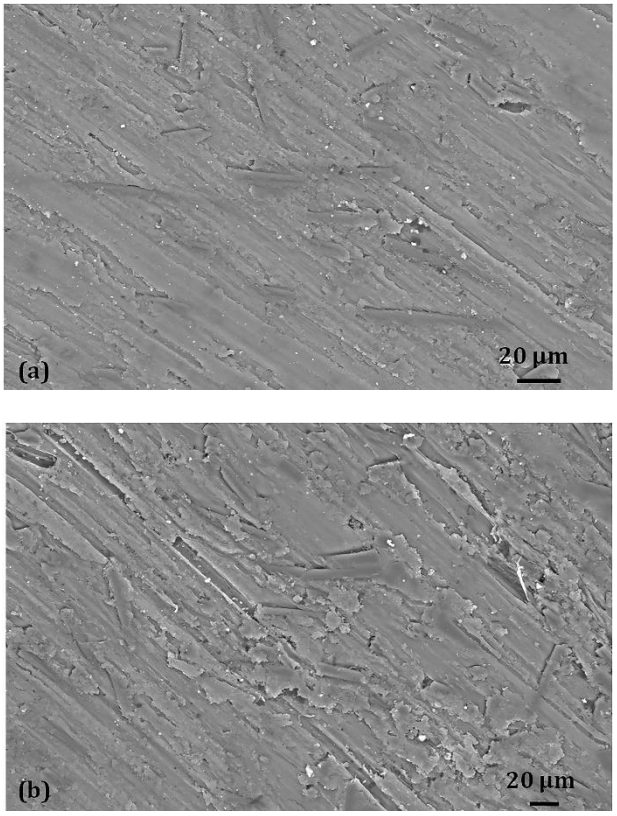


**Fig. 18.** Worn surface of $C_{25}P$ at 750x (a) 4.9 N, 1 m/s (b) 14.7 N, 3 m/s.

SEM image of $C_{25}P$ composite displayed smooth worn surface as shown in Fig. 18(a) when tested with 4.9 N and 1 m/s. However, $C_{25}P$ showed rough surfaces when tested above 14.7 N and 2 m/s. More fibers peeled off from the worn surface can be observed in Fig. 18(b). This could be attributed to the softening of polymer phase due to higher contact temperature and facilitating easy removal of fibers. Hence wear rate increases at higher P and *v* loading conditions. However, once first layer of the fibers removed, melted polymer deposits over the pin surface and forms the counter film. In addition, due to higher thermal conductivity of $C_{25}P$ than neat PES, heat due to friction dissipates faster and prevents excessive wear by melting phenomenon. Hence, wear of $C_{25}P$ composite was lesser than that of neat PES.

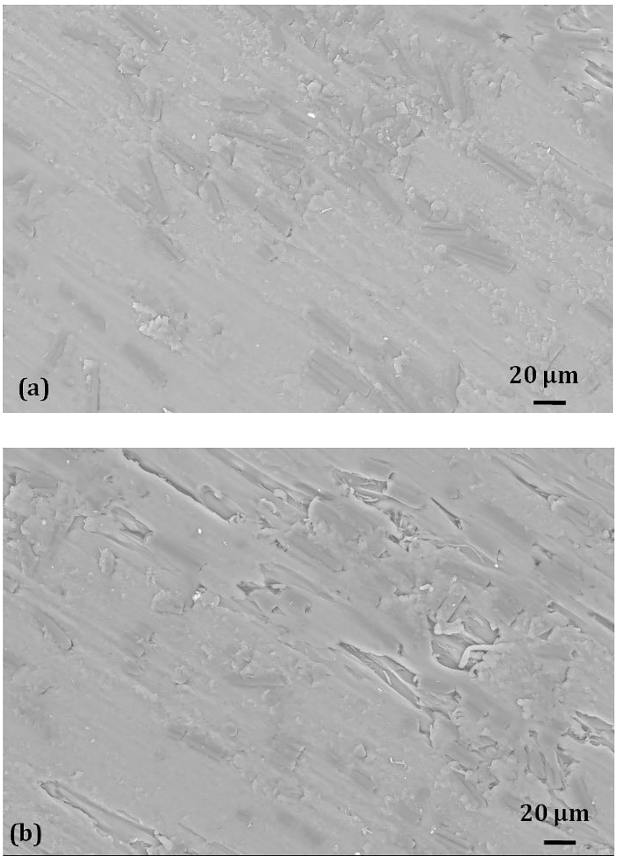


**Fig. 19.** Worn surface of $C_{25}W_{5.0}P$ at 750x (a) 4.9 N, 1 m/s (b) 14.7 N, 3 m/s.

In order to understand how PTW filler helped PES/SCF composite to improve the wear resistance, worn surface of $C_{25}W_{5.0}P$ composite was examined under SEM as shown in Fig. 19. As seen in Fig. 19(a), fibers were found intact in the smooth worn surface when rubbed with 4.9 N and 1 m/s without any fibers peeled off. This suggests that addition of PTW filler improves the wear resistance of $C_{25}W_{2.5}P$ composite. In addition, due to the higher hardness of titanium elements, PTW filled composites showed higher hardness and hence their specific wear rate was decreased. On the other hand, when PTW filled PES/SCF composites were tested with 14.7 N and 3 m/s velocity, more ploughing and plucking of matrix phase was observed around the SCFs and PTW due to much higher contact temperature as noticed in IR images. However, once SCFs were exposed to steel disc, they acted as barrier for wear and prevented further wear loss. This resulted in higher SWR and higher COF. PTW filled composites showed maximum COF compared to all the other developed composites at higher loading conditions. In Fig. 20,

EDX spectrums of (a) pure PES, (b) PES with 25 wt.% of SC, and (c)-(d) PTW filled PES/SCF composites tested under mean loading conditions are presented. Main elements such as carbon, sulphur, oxygen, nitrogen, titanium and potassium were detected as listed in Table 12 in different concentrations according to the amount of fiber/filler reinforced. It was observed that pre-worn neat PES and $C_{25}P$ composites showed carbon content of 58.68% and 66.86% respectively. In contrast, neat PES and $C_{25}P$ composites showed higher carbon content on their worn surfaces which were 64.84% and 77.82% respectively as given in Table 13. This indicates the accumulation of carbon elements on the sliding interface which in turn results in the reduction of COF at the mean loading condition. Among all the developed composites, maximum carbon content was observed on the worn out surface of $C_{25}P$ composite. However, reduction in carbon content was noticed with the addition of PTW filler into the $C_{25}P$ composite. Titanium elements identified on the worn surfaces of PTW filled composites contributed to the enhancement of COF. It is worthwhile to note that titanium metal shows friction coefficient in the range 0.4-0.6 when rubbed against the mild steel counterpart [33]. In addition, due to the higher hardness of titanium elements, PTW filled composites showed higher hardness and hence their specific wear rate was decreased.

**Table 12.** Weight percentage of elements on the pre-worn surfaces.

| Composites | Elements weight (%) | | | | | |
|---|---|---|---|---|---|---|
| | C | O | S | N | Ti | K |
| $C_{00}P$ | 58.68 | 23.34 | 17.98 | - | - | - |
| $C_{25}P$ | 66.86 | 16.74 | 16.39 | 0.01 | | |
| $C_{25}W_{2.5}P$ | 65.22 | 18.75 | 15.94 | 0.02 | 0.04 | 0.03 |
| $C_{25}W_{5.0}P$ | 63.84 | 19.82 | 16.15 | 0.02 | 0.12 | 0.05 |

**Table 13.** Weight percentage of elements on the worn surfaces.

| Composites | Elements weight (%) | | | | | |
|---|---|---|---|---|---|---|
| | C | O | S | N | Ti | K |
| $C_{00}P$ | 64.84 | 16.99 | 18.17 | - | - | - |
| $C_{25}P$ | 77.82 | 12.05 | 10.09 | 0.04 | - | - |
| $C_{25}W_{2.5}P$ | 71.96 | 16.12 | 11.74 | 0.02 | 0.1 | 0.06 |
| $C_{25}W_{5.0}P$ | 68.70 | 16.84 | 13.71 | 0.05 | 0.56 | 0.14 |

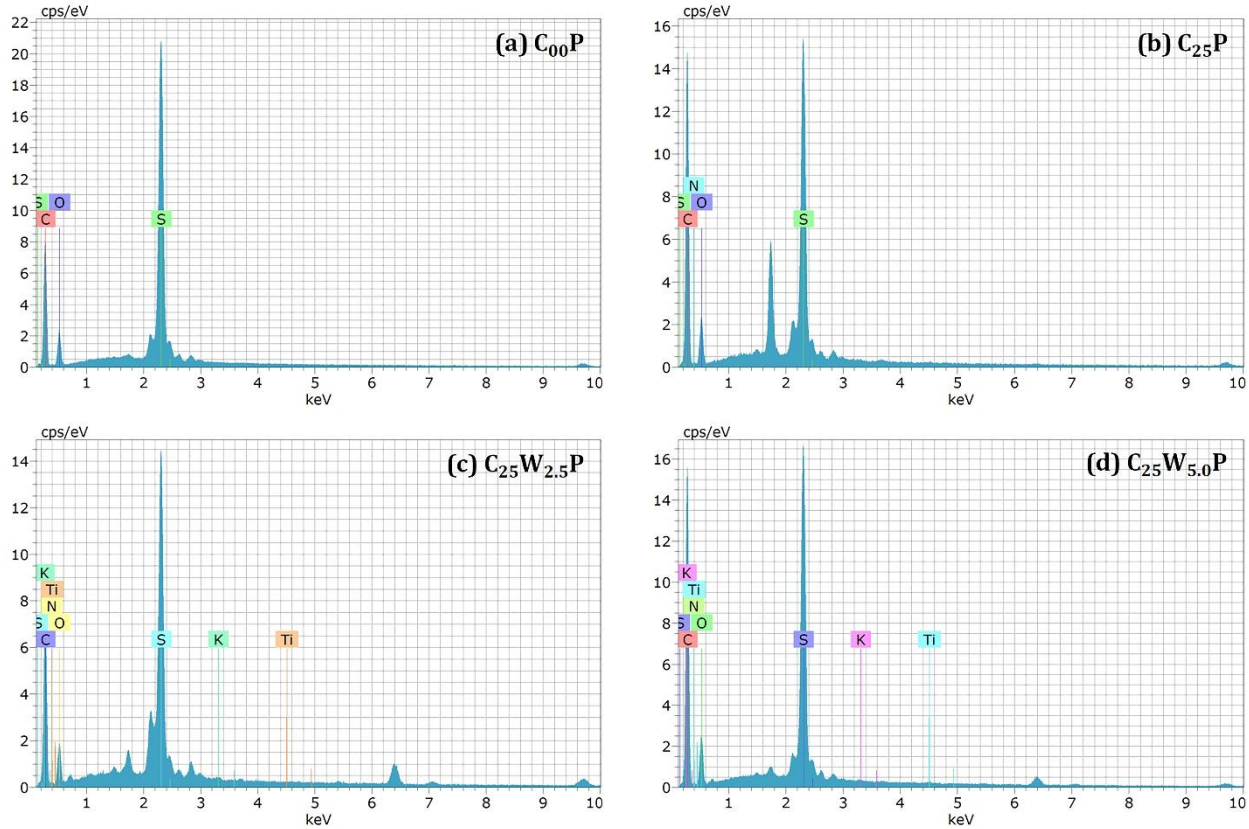


**Fig. 20.** EDS spectrum taken on worn surfaces of filled PES/SCF composites.

## 4. CONCLUSION

PTW was successfully filled into PES/SCF composites by twin screw extruder and injection moulding machine in two different proportions 2.5 and 5 wt. %. Hardness values of PTW filled composites increased. RSM based CCD approach was used to determine, estimate and optimize tribological responses such as COF, SWR and $T_b$ of filled PES/SCF composites. Effect (both individual and interaction) of fiber and/or filler reinforcements, applied load and sliding velocity on COF, SWR and $T_b$ were adequately modelled, optimized, and examined by scanning electron microscope. All the three tribological variables showed significant effect on the SWR, COF and $T_b$ responses. However, main significant factor affecting the SWR and COF was found as

fiber/filler reinforcement followed by applied load and sliding velocity. Linear effects of normal load and sliding velocity dominated the bulk temperature than the fiber/filler content. The predicted COF, SWR and $T_b$ showed good conformability with experimental results. In the case of filled composites, PTW filled composites showed maximum COF and minimum wear. For PTW filled composites, optimum wear conditions were found as 5 wt.% of PTW filler, 15.9 N load and 0.58 m/s sliding velocity. Furthermore, contact temperature monitored during the wear test helped in considering the effect of friction heating on the COF and SWR values. PTW filled composites exhibited higher friction with minimum specific wear rate and hence qualifies for applications such as brake liners.

## Acknowledgement

Injection moulding of the specimens were fully supported by the Brakes India Limited, Sundaram Polymers Division, Nanjangud, Mysore District, Karnataka, India. We wholeheartedly thank Mr. P. Krishna Kumar, Vice President–Operations, and Mr. S. Srinivas, Product Development Department, Brakes India Limited for their support in the fabrication of composites.

## REFERENCES

[1] K. Friedrich, "Polymer composites for tribological applications," *Advanced Industrial and Engineering Polymer Research*, vol. 1, no. 1, pp. 3–39, Oct. 2018, doi: 10.1016/j.aiepr.2018.05.001.

[2] M. Aurilia, L. Sorrentino, L. Sanguigno, and S. Iannace, "Nanofilled polyethersulfone as matrix for continuous glass fibers composites: Mechanical properties and solvent resistance," *Advances in Polymer Technology*, vol. 29, no. 3, pp. 146–160, Sep. 2010, doi: 10.1002/adv.20187.

[3] J. S. Jayan *et al.*, "An introduction to fiber reinforced composite materials," in *Elsevier eBooks*, 2021, pp. 1–24. doi: 10.1016/b978-0-12-821090-1.00025-9.

[4] F. Li *et al.*, "Effectively enhanced mechanical properties of injection molded short carbon fiber reinforced polyethersulfone composites by phenol-formaldehyde resin sizing," *Composites Part B: Engineering*, vol. 139, pp. 216–226, Apr. 2018, doi: 10.1016/j.compositesb.2017.11.033.

[5] F. Li *et al.*, "Enhanced mechanical properties of short carbon fiber reinforced polyethersulfone composites by graphene oxide coating," *Polymer*, vol. 59, pp. 155–165, Feb. 2015, doi: 10.1016/j.polymer.2014.12.067.

[6] A. Zhang, G. Zhao, H. Yang, and Y. Guan, "Mechanical and thermal properties of ABS/PMMA/Potassium Titanate whisker composites," *Polymer-plastics Technology and Engineering*, vol. 56, no. 4, pp. 382–390, Dec. 2016, doi: 10.1080/03602559.2016.1211698.

[7] Z.-K. Zhao *et al.*, "Mechanical and tribological properties of short glass fiber and short carbon fiber reinforced polyethersulfone composites: A comparative study," *Composites Communications*, vol. 8, pp. 1–6, Jun. 2018, doi: 10.1016/j.coco.2018.02.001.

[8] J. Bijwe, J. J. Rajesh, A. Jeyakumar, A. K. Ghosh, and U. S. Tewari, "Influence of solid lubricants and fibre reinforcement on wear behaviour of polyethersulphone," *Tribology International*, vol. 33, no. 10, pp. 697–706, Oct. 2000, doi: 10.1016/s0301-679x(00)00104-3.

[9] Y. L. You, D. X. Li, J. Gao, and X. Deng, "Investigation of the influence of solid lubricants on the tribological properties of polyamide 6 nanocomposite," *Wear*, vol. 311, no. 1–2, pp. 57–64, Mar. 2014, doi: 10.1016/j.wear.2013.12.018.

[10] X. F. Teng, L. Wen, Y. Lv, W. Tang, X. Zhao, and C. Chen, "Effects of potassium titanate whisker and glass fiber on tribological and mechanical properties of PTFE/PEEK blend," *High Performance Polymers*, vol. 30, no. 6, pp. 752–764, Aug. 2017, doi: 10.1177/0954008317723444.

[11] M. Sudheer, R. Prabhu, K. S. R. Raju, and T. N. Bhat, "Effect of filler content on the performance of Epoxy/PTW composites," *Advances in Materials Science and Engineering*, vol. 2014, pp. 1–11, Jan. 2014, doi: 10.1155/2014/970468.

[12] M. Sudheer, R. Prabhu, K. S. R. Raju, and T. N. Bhat, "Optimization of dry sliding wear performance of ceramic whisker filled epoxy composites using Taguchi approach," *Advances in Tribology*, vol. 2012, pp. 1–9, Jan. 2012, doi: 10.1155/2012/431903.

[13] B. Suresha, B. Harshavardhan, and R. Ravishankar, "Tribo-performance of epoxy hybrid composites reinforced with carbon fibers and potassium titanate whiskers," *AIP Conference Proceedings*, Jan. 2018, doi: 10.1063/1.5029645.

[14] X. Zhang, X. Pei, Q. Wang, and T. Wang, "Friction and wear of potassium titanate whisker filled carbon Fabric/Phenolic polymer composites," *Journal of Tribology*, vol. 137, no. 1, Jan. 2015, doi: 10.1115/1.4028911.

[15] H. Wang, Y. Zhu, X. Feng, and X. Lü, "The effect of self-assembly modified potassium titanate whiskers on the friction and wear behaviors of PEEK composites," *Wear*, vol. 269, no. 1–2, pp. 139–144, May 2010, doi: 10.1016/j.wear.2010.03.018.

[16] S. Prabhu, P. H. D. Prasad, and N. Radhika, "Effect of Ni-Coated reinforcement on mechanical and tribological properties of heat treated aluminium composite," *Tribology in Industry*, vol. 42, no. 3, pp. 468–480, Sep. 2020, doi: 10.24874/ti.866.04.20.07.

[17] N. Anjum, B. Suresha, S. L. A. Prasad, and B. Harshavardhan, "Wear Behaviour of Sansevieria and Carbon Fiber Reinforced Epoxy with Nanofillers: Taguchi Method," *Tribology in Industry*, vol. 42, no. 3, pp. 443–460, Sep. 2020, doi: 10.24874/ti.861.03.20.06.

[18] M. J. I. Raj, K. Manisekar, and M. Gupta, "Central composite experimental design applied to the dry sliding wear behavior of MG/Mica composites," *Journal of Tribology*, vol. 141, no. 1, Aug. 2018, doi: 10.1115/1.4041073.

[19] N. Radhika and R. Raghu, "Prediction of mechanical properties and modeling on sliding wear behavior of LM25/TiC composite using response surface methodology," *Particulate Science and Technology*, vol. 36, no. 1, pp. 104–111, Sep. 2016, doi: 10.1080/02726351.2016.1223773.

[20] Q. Sun and W. Li, *Inorganic-Whisker-Reinforced Polymer Composites, Synthesis, Properties and Applications*, CRC Press, New York, SAD, 2016.

[21] B. Harshavardhan, R. Ravishankar, B. Suresha, and S. Srinivas, "Static and dynamic mechanical performance of carbon fiber reinforced polyethersulfone composites," *Applied Mechanics and Materials*, vol. 895, pp. 265–271, Nov. 2019, doi: 10.4028/www.scientific.net/amm.895.265.

[22] "Veradel PESU." https://www.solvay.com/en/brands/veradel-pesu

[23] "Chopped fiber: Teijin carbon." https://www.teijincarbon.com/products/short-fibers/chopped-fibers/

[24] "Titanates-for-plastics" https://noblealchem.com/titanates-for-plastics

[25] *Standard Test Methods for Density and Specific Gravity (Relative Density) of Plastics by Displacement*, ASTM D792-20, 2015.

[26] *Standard Test Method for Indentation Hardness of Rigid Plastics by Means of a Barcol Impressor*, ASTM D2583-06, 2013.

[27] *Standard Test Method for Wear Testing with a Pin-on-Disk Apparatus*, ASTM G99-17,2015.

[28] G. Xie, G. Zhuang, G. Sui, and R. Yang, "Tribological behavior of PEEK/PTFE composites reinforced with potassium titanate whiskers," *Wear*, vol. 268, no. 3–4, pp. 424–430, Feb. 2010, doi: 10.1016/j.wear.2009.08.032.

[29] B. Harshavardhan, R. Ravishankar, B. Suresha, S. Srinivas, and U. A. C. Dixit, "Thermal characterization of polyethersulfone composites filled with self lubricants," *Materials Today: Proceedings*, vol. 43, pp. 1258–1267, Jan. 2021, doi: 10.1016/j.matpr.2020.08.768.

[30] K. Friedrich, *Friction and wear of polymer composites*, Elsevier New York, SAD, 1986.

[31] N. Sh. El-Gendy, H. R. Madian, and S. S. A. Amr, "Design and Optimization of a process for sugarcane molasses fermentation bySaccharomyces CerevisiaeUsing Response Surface Methodology," *International Journal of Microbiology*, vol. 2013, pp. 1–9, Jan. 2013, doi: 10.1155/2013/815631.

[32] R. Ghelich, M. R. Jahannama, H. Abdizadeh, F. S. Torknik, and M. Vaezi, "Central composite design (CCD)-Response surface methodology (RSM) of effective electrospinning parameters on PVP-B-Hf hybrid nanofibrous composites for synthesis of HfB2-based composite nanofibers," *Composites Part B: Engineering*, vol. 166, pp. 527–541, Jun. 2019, doi: 10.1016/j.compositesb.2019.01.094.

[33] B. Bhushan, *Principles and applications of tribology*, Wiley, UK, 2013.